

# Structure–Function Relationships in High-Density Octadecylsilane Stationary Phases by Raman Spectroscopy. 4. Effects of Neutral and Basic Aromatic Compounds

Christopher J. Orendorff, Michael W. Ducey, Jr.,<sup>†</sup> and Jeanne E. Pemberton\*

University of Arizona, Department of Chemistry, Tucson, Arizona 85721

Lane C. Sander

National Institute of Standards and Technology, Gaithersburg, Maryland 20899

**The effects of aromatic compounds (toluene, benzene, *p*-xylene, anisole, aniline, and pyridine), temperature, and surface grafting method (surface- or solution-polymerized) on alkyl chain rotational and conformational order in a series of high-density octadecylsilane stationary phases ranging in surface coverage from 3.09 to 6.45  $\mu\text{mol}/\text{m}^2$  are examined by Raman spectroscopy. Rotational and conformational order are assessed using the intensity ratio of the antisymmetric to symmetric  $\nu(\text{CH}_2)$  modes as well as the frequency at which the symmetric  $\nu(\text{CH}_2)$  band is observed. Alkyl rotational and conformational order decrease with decreasing surface coverage in these aromatic compounds, which is consistent with the behavior of these materials in air and in other solvents. In addition, order of the alkyl chains is dependent on solvent hydrophobicity, hydrogen-bonding ability, and basicity. The most hydrophobic compounds impart disorder to the stationary phase; the hydrogen-bonding aromatics increase the rotational order of homogeneously distributed, high-surface-coverage materials; and basic aromatic compounds increase the conformational order of high- and low-coverage materials as the basic compounds undergo silanophilic interactions with exposed surface silanols. From these observations, molecular pictures of the chromatographic interface that display interactions between the alkyl chains and these aromatic compounds are proposed.**

Separation in reversed-phase liquid chromatography (RPLC) is often based on small differences in polarity of analytes within a class of compounds. This is observed by the separation of countless classes of small molecules, including the popular separations of substituted aromatic compounds as standards to determine column performance.<sup>1–3</sup> Substituted aromatics are

structural components of environmentally, pharmacologically, and biologically interesting molecules, including polycyclic aromatic hydrocarbons (PAHs), polychlorinated biphenyl congeners (PCBs), and steroids. Furthermore, substituted aromatics of varying polarity are used to probe fundamental interactions in RPLC. Thus, investigation of solute–stationary-phase and solvent–solute interactions involving these core aromatic systems under chromatographic conditions would lead to a greater understanding of the molecular basis of their retention as well as the retention of more complex aromatic-containing analytes.

As part of previous Raman spectral studies on the effects of polar and nonpolar solvents on the conformational order of high-density alkylsilane stationary phases,<sup>4,5</sup> spectral data were acquired for two nonpolar, aromatic solvents, benzene and toluene. Interestingly, the addition of the methyl group in toluene results in significant changes in interaction with these high-density stationary phases relative to benzene. In general, these stationary phases are at least as disordered, if not more disordered, in toluene as compared to benzene at all temperatures, although this behavior varies with surface coverage and alkylsilane surface homogeneity.<sup>5</sup> In this report, the effects on conformational order of these high-density stationary-phase materials of the neutral and basic aromatic compounds benzene, toluene, *p*-xylene, anisole, aniline, and pyridine are investigated using Raman spectroscopy. Although only benzene and toluene are prominent in RPLC as mobile-phase components and mobile-phase additives, all five of these solutes are more common analytes in RPLC. In particular, the behavior of the basic aromatic compounds is important because of the analytical problems produced by substantial peak tailing in reversed-phase separation of basic analytes of pharmaceutical or forensic interest.

This work is one in a series of publications that represent a continuing effort to understand the molecular basis of chromato-

\* To whom correspondence should be addressed. Phone: (520) 621-8245. E-mail: pemberton@u.arizona.edu.

<sup>†</sup> Current address: Department of Chemistry, Missouri Western State College, St. Joseph, MO 64507.

(1) Khong, T. M.; Simpson, C. F. *Chromatographia* **1987**, *24*, 385–394.

(2) Smith, R. M.; Burr, C. M. *J. Chromatogr.* **1989**, *475*, 57–74.

(3) Tanaka, N.; Kimata, K.; Hosoya, K.; Miyazishi, H.; Takeo, A. *J. Chromatogr., A* **1993**, *656*, 265–287.

(4) Pemberton, J. E.; Ho, M.; Orendorff, C. J.; Ducey, M. W. *J. Chromatogr., A* **2001**, *913*, 243–252.

(5) Ducey, M. W.; Orendorff, C. J.; Pemberton, J. E.; Sander, L. C. *Anal. Chem.* **2002**, *74*, 5585–5592.

Table 1. Octanol–Water Partition Coefficients for Aromatic Compounds<sup>a</sup>

compd	log $K_{ow}$
pyridine	0.65
aniline	0.90
anisole	2.11
benzene	2.13
toluene	2.73
<i>p</i> -xylene	3.15

<sup>a</sup> From references 12, 13.

graphic retention though deduction of complex analyte–solute–stationary-phase interactions. The first three reports in this series described the inter- and intramolecular interactions within the stationary phase<sup>6</sup> and solvent–stationary-phase interactions,<sup>5,7</sup> respectively. The work in this report represents the necessary first step toward elucidating solute–stationary-phase interactions through investigation of such interactions in neat solutions of the solute. Thus, although not strictly relevant as chromatographic conditions, these studies provide the foundation for interpretation of solute–stationary-phase interactions at chromatographically relevant concentrations in the presence of mobile-phase solvent.

## EXPERIMENTAL SECTION<sup>1</sup>

**Materials.** Octadecylsilane-modified silica-based stationary phases were prepared and characterized as previously described;<sup>8,9</sup> the specifications of these stationary phases, including surface coverage, were listed in Table 1 of the preceding paper in this Journal.<sup>7</sup> Perdeuterated solvents (benzene, toluene, *p*-xylene, anisole, aniline, and pyridine) were obtained from Cambridge Isotope Laboratories and were used as received.

**Procedures.** Samples were prepared by placing between 25 and 100 mg of stationary-phase material into a 5-mm-diameter NMR tube; 200  $\mu$ L of solvent was then added. Samples were sonicated for 10 min and equilibrated at 20 °C for a minimum of 12 h prior to spectral acquisition. Raman spectra were collected, processed, and analyzed using the same procedures described in the preceding paper in this Journal.<sup>7</sup>

**Molecular Pictures.** Models of the solvent–stationary-phase interface were constructed and energy-minimized using the same software and mathematical parameters as described in the preceding paper in this Journal.<sup>7</sup>

## RESULTS AND DISCUSSION

**Raman Spectroscopy of High-Density Alkylsilane Stationary Phases in Solvent.** Typical spectra in the  $\nu(\text{C–H})$  region (2750–3050  $\text{cm}^{-1}$ ) for all five high-density stationary-phase materials at room temperature in toluene and anisole are shown in Figure 1. The corresponding peak frequencies and vibrational mode assignments are given in Table 3 of the preceding paper in this Journal.<sup>7</sup> Raman spectra in the  $\nu(\text{C–H})$  region for these stationary

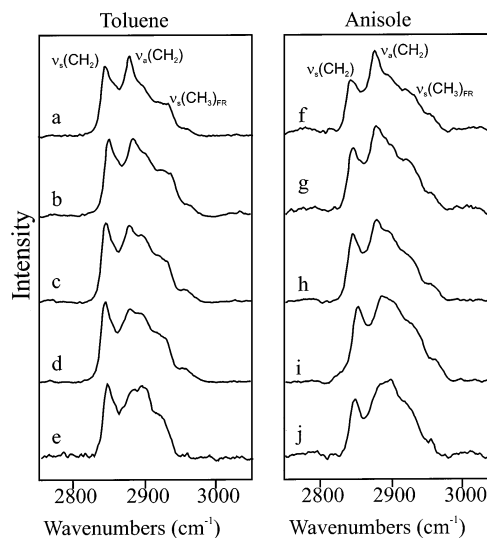


Figure 1. Raman spectra in the  $\nu(\text{C–H})$  region for (a, f) TFC18SF, (b, g) TFC18SL, (c, h) DFC18SF, (d, i) DFC18SL, and (e, j) MFC18 in perdeuterated toluene (left panel) and anisole (right panel) at 20 °C. Spectral acquisition times for TFC18SF, TFC18SL, DFC18SF, and DFC18SL in all solvents are 2 min. Spectral acquisition times for MFC18 in all solvents are 5 min.

phases in the other four media (benzene, aniline, pyridine, and *p*-xylene) are provided in the Supporting Information in Figures S1 and S2.

The basis for interpretation of the Raman spectral results for surface-bound alkylsilanes in the  $\nu(\text{C–H})$  region using the intensity ratio of the  $\nu_a(\text{CH}_2)$  to the  $\nu_s(\text{CH}_2)$  [ $I[\nu_a(\text{CH}_2)]/I[\nu_s(\text{CH}_2)]$ ] and the  $\nu_a(\text{CH}_2)$  and  $\nu_s(\text{CH}_2)$  peak frequencies is discussed in the preceding paper in this Journal.<sup>7</sup>

**Effects of Aromatic Compounds on High-Density Stationary-Phase Order.** In previous reports,<sup>5,7</sup> solvent–stationary-phase interactions for these high-density materials were quantified by the solvatochromic parameter,  $\pi^*$ , as described by Kamlet.<sup>11</sup> In this report, however, because these aromatic compounds can be viewed as both solvent and solute in chromatographic systems, we have chosen not to limit the description of these systems to solvents, but rather to describe them in terms of octanol–water partition coefficients ( $\log K_{ow}$ ) which are measures of hydrophobicity applicable to both solvents and solutes.  $K_{ow}$  values for the aromatic systems studied here are tabulated in Table 1.<sup>12,13</sup>

In Figure 2,  $I[\nu_a(\text{CH}_2)]/I[\nu_s(\text{CH}_2)]$  is plotted as a function of  $\log K_{ow}$  for all five stationary phases in neat solutions of each aromatic compound at 20 °C. In general,  $I[\nu_a(\text{CH}_2)]/I[\nu_s(\text{CH}_2)]$  increases with increasing alkylsilane surface coverage in these neat aromatic compounds. This behavior is identical to that observed for these materials in air, polar solvents, and nonpolar solvents.<sup>5–7</sup> In addition,  $I[\nu_a(\text{CH}_2)]/I[\nu_s(\text{CH}_2)]$  varies with hydrophobicity and polarity of these aromatic compounds. With the exception of anisole, which clearly exhibits anomalous behavior as discussed below, the  $I[\nu_a(\text{CH}_2)]/I[\nu_s(\text{CH}_2)]$  values for the high-coverage, homogeneous stationary phases (TFC18SF and

(6) Ducey, M. W.; Orendorff, C. J.; Pemberton, J. E.; Sander, L. C. *Anal. Chem.* **2002**, *74*, 5576–5584.

(7) Orendorff, C. J.; Ducey, M. W.; Pemberton, J. E.; Sander, L. C. *Anal. Chem.* **2003**, *75*, 3360–3368.

(8) Sander, L. C.; Wise, S. A. *Anal. Chem.* **1995**, *67*, 3284–3292.

(9) Pursch, M.; Sander, L. C.; Albert, K. *Anal. Chem.* **1996**, *68*, 4107–4113.

(10) Thompson, W. R.; Pemberton, J. E. *Anal. Chem.* **1994**, *66*, 3362–3370.

(11) Kamlet, M. J.; Abboud, J. M.; Abraham, M. H.; Taft, R. W. *J. Org. Chem.* **1983**, *48*, 2877–2887.

(12) Hansch, C.; Leo, A. *Substituent Constants for Correlation Analysis in Chemistry and Biology*; Wiley: New York, 1979.

(13) Sangster, J. *J. Phys. Chem. Ref. Data* **1989**, *18*, 1111–1229.

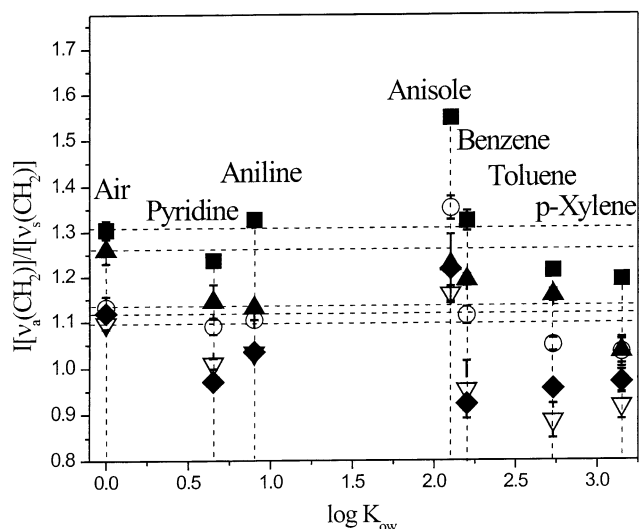


Figure 2.  $I[v_a(\text{CH}_2)]/I[v_s(\text{CH}_2)]$  as a function of  $\log K_{ow}$  for TFC18SF (■), TFC18SL (▲), DFC18SF (○), DFC18SL (◆), and MFC18 (▽) in air, *p*-xylene, toluene, benzene, anisole, aniline, and pyridine. Error bars represent one standard deviation (experimental).

DFC18SF) are fairly constant with increasing hydrophobicity ( $\log K_{ow}$ ) for air, pyridine, and benzene, and then decrease slightly with increasing  $\log K_{ow}$  from benzene to *p*-xylene. For TFC18SL,  $I[v_a(\text{CH}_2)]/I[v_s(\text{CH}_2)]$  decreases relative to air for all aromatics, especially *p*-xylene. For DFC18SL and MFC18,  $I[v_a(\text{CH}_2)]/I[v_s(\text{CH}_2)]$  decreases relative to air for all aromatics, with the disorder generally increasing with  $\log K_{ow}$ .

In the most hydrophobic, nonpolar aromatic compounds, toluene and *p*-xylene, the values of  $I[v_a(\text{CH}_2)]/I[v_s(\text{CH}_2)]$  for all five stationary phases are the lowest of all of the aromatic compounds investigated, suggesting the least conformational order of the alkyl chains. These observations are rationalized in terms of greater interaction of these hydrophobic compounds with the alkyl chains. Indeed, the significant values of the dissolution enthalpies for toluene and *p*-xylene in hexadecane<sup>14</sup> of  $-8.58$  and  $-9.89$  kcal/mol, respectively, support the interpretation of this behavior in terms of deep penetration (i.e., partitioning in the chromatographic sense) of these aromatics into the alkylsilanes. The methyl substituents on each of these compounds confers additional hydrophobicity relative to benzene, for example, that facilitates this deeper penetration.

The effect of benzene on the order of these materials is more dependent on surface coverage than the effect of either toluene or *p*-xylene. MFC18 and DFC18SL are significantly more disordered in benzene than in air, and TFC18SL and DFC18SF are slightly more disordered in benzene than in air, but TFC18SF is relatively unchanged in benzene relative to air.

Interestingly, all stationary phases except TFC18SL are significantly more ordered in anisole than in air at 20 °C. Similar ordering has previously been observed for TFC18SF and DFC18SF in self-associating solvents (e.g., methanol, ethanol, acetic acid, and acetonitrile)<sup>7</sup> and has been attributed to self-association of solvent molecules at the distal methyl end of the alkylsilane chains in a manner that actually increases chain order. This ordering

phenomenon has been observed exclusively for stationary phases composed of alkyl chains that are both high in surface coverage and homogeneously distributed across the silica surface (as determined by NMR spectroscopy<sup>9</sup>).

In anisole, not only are the two high-coverage, homogeneous materials ordered relative to air, but the materials with lower surface coverage are ordered relative to air, as well. Anisole is known to strongly self-associate through hydrogen-bonding interactions at the oxygen atom.<sup>15</sup> Thus, a picture similar to that proposed earlier for other systems in which self-association of the solvent at the distal methyl end of the alkyl chains holds the chains together is adequate to account for ordering of the high-coverage, homogeneous stationary phases. However, the observation of anisole-induced ordering of the heterogeneous, low-coverage materials MFC18 and DFC18SL was initially puzzling, since other self-associating solvents, such as ethanol, do not order these stationary phases. If one considers differences in solubility behavior and structure between anisole and ethanol, for example, the difference in ordering of these phases in these two media becomes clear. On the basis of the considerably larger octanol–water partition coefficient for anisole ( $\log K_{ow} = 2.11$ ) relative to ethanol ( $\log K_{ow} = -0.30$ ) and the larger enthalpy of dissolution in hexadecane of anisole ( $\Delta H_s = -9.90$  kcal/mol) relative to ethanol ( $\Delta H_s = -3.90$  kcal/mol),<sup>12–14</sup> one would predict that the interaction of anisole with the stationary phase should be greater than that of ethanol. In part, the difference in enthalpy of dissolution is due to the much larger size of anisole ( $V_m = 0.108$  nm<sup>3</sup>) relative to ethanol ( $V_m = 0.053$  nm<sup>3</sup>).<sup>16,17</sup> However, even when corrected for these molecular volume differences, the dissolution of anisole in hexadecane ( $\Delta H_s/V_m = -92$  kcal/mol·nm<sup>3</sup>) is favored over the dissolution of ethanol in hexadecane ( $\Delta H_s/V_m = -74$  kcal/mol·nm<sup>3</sup>). This strong interaction, a result of solubility and structural characteristics, coupled with the ability of anisole to self-associate at the stationary-phase–solvent interface, provide favorable energetics for both the high- and low-coverage stationary phases to order in anisole relative to air.

Although aniline and pyridine are significantly more hydrophilic than the other four aromatic compounds, as indicated by their  $\log K_{ow}$  values, the values of  $I[v_a(\text{CH}_2)]/I[v_s(\text{CH}_2)]$  in these solvents are low, suggesting that they penetrate deeply into the alkyl chains and impart significant disorder to these alkylsilanes. For aniline and pyridine, this partitioning into the alkyl chains should be thermodynamically comparable to that of the other hydrophobic aromatics on the basis of their enthalpies of dissolution in hexadecane ( $\Delta H_s$  (aniline) =  $-9.99$  kcal/mol,  $\Delta H_s$  (pyridine) =  $-7.80$  kcal/mol).<sup>14</sup> Indeed, one might predict slightly less interaction of pyridine with the alkyl chains on the basis of its slightly less favorable enthalpy. In contrast to this prediction, however, these stationary phases are generally slightly more disordered in pyridine than aniline. This behavior is proposed to be due to the additional driving force for partitioning of pyridine due to hydrogen-bonding with unreacted surface silanols (also called silanophilic interactions), which results in peak tailing in

(14) Abraham, M. H.; Whiting, G. S.; Fuchs, R.; Chambers, E. J. *J. Chem. Soc., Perkin Trans 2* **1990**, 2, 291–300.

(15) Nobeli, I.; Yeoh, S. L.; Price, S. L.; Taylor, R. *Chem. Phys. Lett.* **1997**, 280, 196–202.

(16) Kitaigorodski, A. I. *Organic Chemical Crystallography*; Consultants Bureau: New York, 1961.

(17) Molecular volumes estimated from values in Gavezzotti, A. *J. Am. Chem. Soc.* **1983**, 105, 5220–5225.



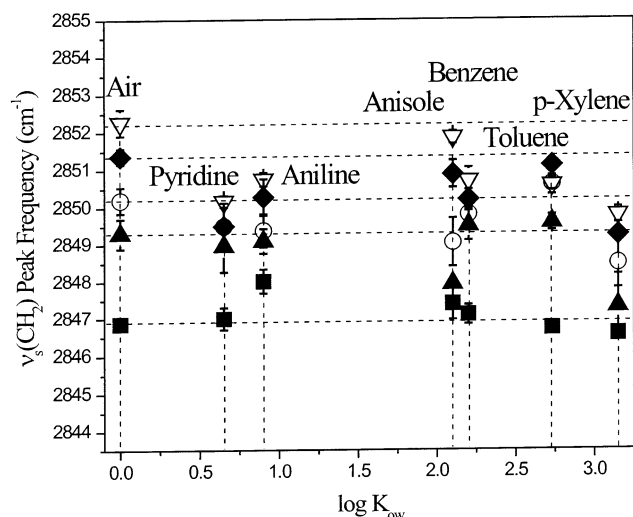


Figure 3.  $\nu_s(\text{CH}_2)$  peak frequency as a function of  $\log K_{\text{ow}}$  for TFC18SF (■), TFC18SL (▲), DFC18SF (○), DFC18SL (◆), and MFC18 (▽) in air, *p*-xylene, toluene, benzene, anisole, aniline, and pyridine. Error bars represent one standard deviation (experimental).

chromatographic experiments.<sup>18–21</sup> Pyridine is a slightly stronger base than aniline [ $K_a$  (pyridine) = 5.23,  $K_a$  (aniline) = 4.60] which increases its hydrogen-bonding to surface silanols.

The effect of these additional Brønsted acid–base interactions is expected to be a function of the number of unreacted surface silanols, which scales inversely with alkylsilane surface coverage. The increased conformational disorder of TFC18SF, in which the number of unreacted surface silanols is low, in pyridine relative to aniline is attributed to its slightly greater base strength and smaller molecular size. For the other stationary phases, lower alkylsilane surface coverage allows substantial access to surface silanols, and the conformational order of these materials in aniline and pyridine is approximately equivalent. Unfortunately, the expected shifts due to hydrogen-bonding in the silanol  $\nu(\text{O}-\text{H})$  and the perdeuterated aniline  $\nu(\text{N}-\text{D})$  modes cannot be observed as a result of spectral interference from the bulk solvent and silica. Nonetheless, even without direct Raman spectral evidence to support hydrogen-bonding of these species, the plethora of chromatographic data that identify silanophilic interactions for basic analytes support this interpretation of the conformational order of alkylsilanes in these systems.<sup>18–21</sup>

In addition to the conformational order information obtained from  $I[\nu_a(\text{CH}_2)]/I[\nu_s(\text{CH}_2)]$  values, the effect of aromatic compounds on alkyl chain coupling in these high-density stationary phases can be determined from the  $\nu_s(\text{CH}_2)$  peak frequency. Figure 3 is a plot of  $\nu_s(\text{CH}_2)$  peak frequency as a function of  $\log K_{\text{ow}}$  for these stationary phases in perdeuterated *p*-xylene, toluene, benzene, anisole, aniline, and pyridine. As seen for these materials in air and in other solvents, the  $\nu_s(\text{CH}_2)$  peak frequency depends on surface coverage in these aromatic compounds, generally increasing with decreasing surface coverage. For the highest coverage materials, the  $\nu_s(\text{CH}_2)$  peak frequency is generally constant with  $\log K_{\text{ow}}$ . However, for MFC18, the  $\nu_s(\text{CH}_2)$  peak

frequency increases with increasing  $\log K_{\text{ow}}$  from pyridine to anisole, and then decreases from anisole to *p*-xylene.

For TFC18SF, aromatic compounds have very little effect on alkyl chain coupling. For the intermediate coverage materials, TFC18SL and DFC18SF, appreciable disorder in *p*-xylene relative to air is suggested by the value of  $I[\nu_a(\text{CH}_2)]/I[\nu_s(\text{CH}_2)]$ ; however, the  $\nu_s(\text{CH}_2)$  peak frequencies for these systems in *p*-xylene suggests greater alkyl chain coupling in *p*-xylene relative to air, despite the apparent conformational disorder. The contradiction between these two spectral indicators, albeit atypical, may not be too surprising considering that they are measures of two separate parameters.<sup>22</sup> Nonetheless, this apparent discrepancy indicates the need for a more systematic study of the relationship between chain coupling and conformational order in these alkylsilane systems, as would be accessible by access to a larger number of spectral indicators, especially those in the frequency region containing information about true gauche C–C bonds. Given that the inherent fluorescence of the silica substrates on which these materials are based precludes access to this region of the spectrum, the resolution of this discrepancy awaits the fabrication of a similar series of systems on nonfluorescent silica. We hope to undertake the fabrication of such systems and will report our spectral findings on these systems at a later date.

For the lowest coverage materials, DFC18SL and MFC18, the alkyl chains are more coupled in aromatic compounds than in air. In anisole, the increase in chain coupling is not as great in the disordering aromatic solvents. For stationary phases with intermediate and low surface coverages (3.09–5.26  $\mu\text{mol}/\text{m}^2$ ), alkyl chains are more coupled in these aromatic compounds than in air at room temperature. For the high coverage materials, interaction at the distal end of the alkyl chains decreases coupling at the end of the alkyl chains.

The conformational order and chain-coupling information obtained from the Raman spectroscopy of these high-density stationary phases in aromatic compounds allow development of detailed molecular pictures of the solvent–stationary-phase interface. These pictures were created with ChemDraw3D using energy-minimized MM2 computations on a small matrix of alkylsilanes. The proposed pictures of these interfacial interactions are shown in Figure 4a–d for TFC18SF in anisole, and MFC18 in anisole, aniline, and toluene, respectively, as representative of the various interactions proposed for high- and low-coverage materials in these aromatic compounds. The interaction of anisole at the distal methyl group of the alkyl chains of TFC18SF and MFC18 allows lateral ordering of the anisole molecules through hydrogen-bonding. Moreover, this interaction induces conformational ordering of the alkyl chains with slight decoupling of the distal portion for the closely packed TFC18SF but slight coupling of the distal end of the chains for MFC18. For MFC18 in aniline, it is proposed that the high fraction of exposed surface silanols causes penetration of aniline molecules to the silica surface to establish hydrogen-bonds. As a result, the alkyl chains are slightly more disordered than in air because of the cavity formed to accommodate the aniline molecules at the surface, even though these chains couple at the distal end away from the silica surface. For MFC18 in toluene, significant disorder is imparted to the alkyl

(18) Nahum, A.; Horvath, C. *J. Chromatogr.* **1981**, *203*, 53–63.

(19) Gill, R.; Alexander, S. P.; Moffat, A. C. *J. Chromatogr.* **1982**, *247*, 39–45.

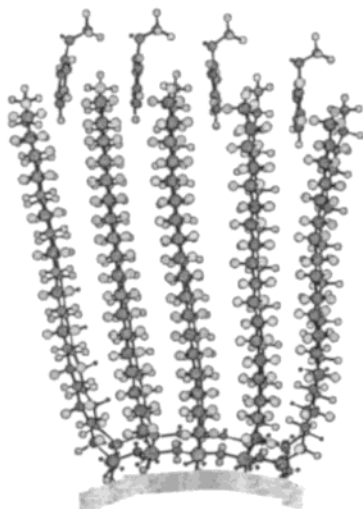
(20) Sekulic, S.; Haddad, P. R. *J. Chromatogr.* **1988**, *459*, 65–77.

(21) McCalley, D. V. *J. Chromatogr.* **1993**, *636*, 213–220.

(22) Orendorff, C. J.; Ducey, M. W.; Pemberton, J. E. *J. Phys. Chem. A* **2002**, *106*, 6991–6998.

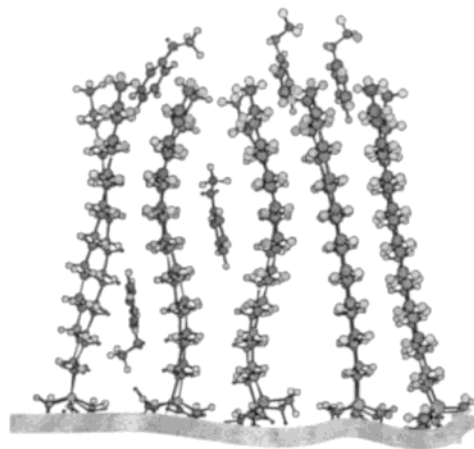
TFC18SF in Anisole

a



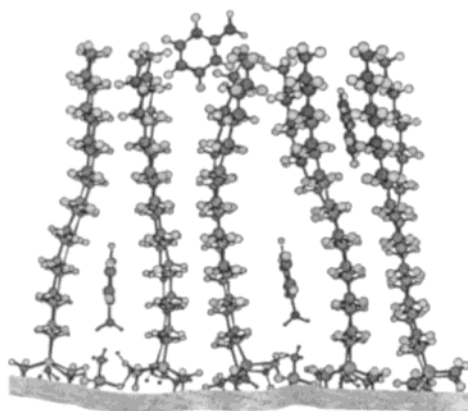
MFC18 in Anisole

b



MFC18 in Aniline

c



MFC18 in Toluene

d

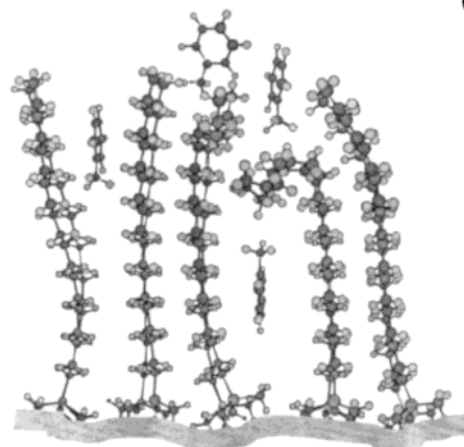


Figure 4. Alkylsilane interfaces from MM2 energy-minimized computations for (a) anisole at TFC18SF, (b) anisole at MFC18, (c) aniline at MFC18, and (d) toluene at MFC18.

chains, with the retention of large portions of coupled alkyl chains.

**Effects of Temperature.** Examination of the effects of temperature and solvent on the conformational order of these high-density stationary phases extends our understanding of the complex interactions of these materials with aromatic compounds as both solvents and solutes in chromatographic systems. Figure 5 shows plots of  $I[\nu_a(\text{CH}_2)]/I[\nu_s(\text{CH}_2)]$  and  $\nu_s(\text{CH}_2)$  peak frequency as a function of temperature for TFC18SF (Figure 5a and b) and MFC18 (Figure 5c and d) in *p*-xylene, toluene, benzene, anisole, aniline, and pyridine. For TFC18SF (Figure 5a), temperature-induced disordering of the alkyl chains is generally observed, with a convergence at high temperature to a minimum value of  $I[\nu_a(\text{CH}_2)]/I[\nu_s(\text{CH}_2)]$ . The exception to this behavior for TFC18SF is anisole, in which the alkyl chains remain more ordered at high temperatures than in the other aromatics. In addition, a small degree of temperature-induced chain decoupling is observed for TFC18SF in all compounds with convergence to a maximum decoupled state at high temperatures (Figure 5b).

For MFC18, conformational order is much less temperature-dependent for toluene and benzene and is essentially independent of temperature for anisole, pyridine, and aniline. Similarly, alkyl chain decoupling for MFC18 is exclusively solvent-dependent for all aromatic compounds, with the exception of *p*-xylene. This interplay between solvent- and temperature-induced disordering and chain decoupling as a function of surface coverage is consistent with observations made for these stationary phases in polar and nonpolar solvents.<sup>5,7</sup> Similar trends are observed for the intermediate surface coverage materials, TFC18SL, DFC18SF, and DFC18SL, as indicated by the corresponding plots (Figures S3 and S4) in the Supporting Information.

At low temperatures, all stationary phases are more ordered in *p*-xylene than in any other aromatic compound or, indeed, in any solvent from previous investigations.<sup>5,8</sup> Neat *p*-xylene freezes at  $\sim 13^\circ\text{C}$ , and the sample visually appears to be a crystalline solid at temperatures  $< 5^\circ\text{C}$ . Lowering the temperature after the room temperature addition of *p*-xylene to the stationary phase freezes

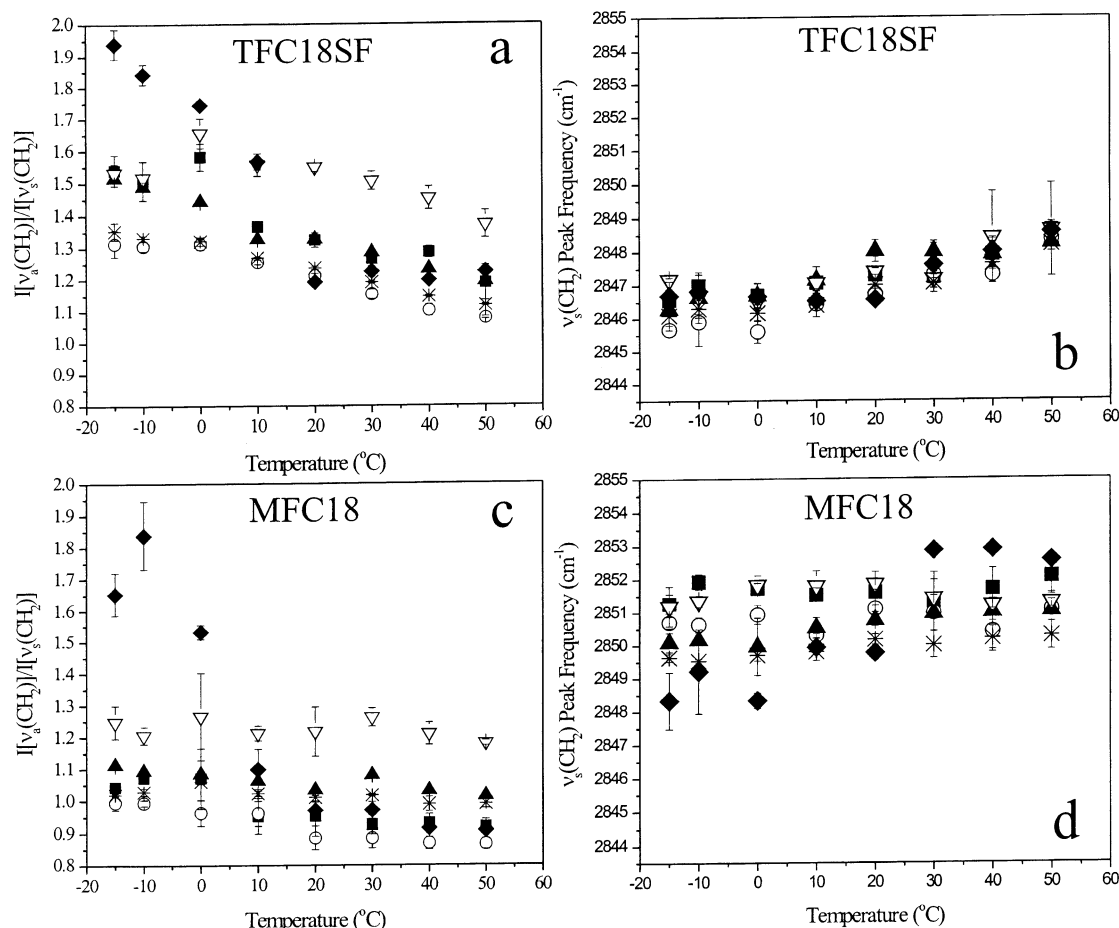


Figure 5. Temperature-dependence of  $I[\nu_a(\text{CH}_2)]/I[\nu_s(\text{CH}_2)]$  for (a) TFC18SF and (c) MFC18 and  $\nu_s(\text{CH}_2)$  peak frequency for (b) TFC18SF and (d) MFC18 in benzene (■), aniline (▲), toluene (○), *p*-xylene (◆), anisole (▽), and pyridine (\*). Error bars represent one standard deviation (experimental).

the *p*-xylene and the solvated stationary phase, resulting in a highly ordered state that exhibits slightly less chain coupling than in neat crystalline hydrocarbons (e.g., octadecane, polyethylene).<sup>22</sup> Once the temperature is sufficiently elevated to melt the *p*-xylene–stationary-phase system, *p*-xylene–alkyl chain interactions predominate, and significant disorder and chain decoupling is imparted to the stationary phase.

## CONCLUSIONS

A detailed examination of interactions between aromatic compounds and high-density stationary phases probed by Raman spectroscopy is presented. Results indicate that conformational order of these materials is a function of the degree and nature of the aromatic substituents and how these substituents impact the properties of the aromatic compound (e.g., polarity, hydrophobicity, steric bulk, hydrogen-bonding ability). Interaction of the hydrophobic aromatic compounds benzene, toluene, and *p*-xylene with these stationary phases is best described in terms of a partitioning model in which significant disorder is imparted to these stationary-phase alkyl chains. The interaction of the basic aromatic compounds aniline and pyridine with these phases is proposed to reflect a combination of hydrophobic interactions with the alkyl chains and silanophilic interactions with silanols on the silica surface. Unfortunately, direct Raman spectral evidence for these silanophilic interactions is unavailable because of the small

number of surface hydrogen-bonded molecules relative to those in the bulk, although such interactions are clearly supported by chromatographic data for basic compounds. Anisole interacts with the distal portions of these phases in a manner that allows lateral hydrogen-bonding at the methoxy oxygen atom between anisole molecules and induces conformational ordering of the alkyl chains.

Future reports in this series of publications detailing the use of Raman spectroscopy for the elucidation of detailed molecular information about RPLC stationary-phase materials will explore the effects of mixed solvent/solute systems, with the goal of elucidating retention mechanisms in chromatographically relevant systems. These studies are currently in progress and will be reported at a later date.<sup>23,24</sup>

## ACKNOWLEDGMENT

The authors gratefully acknowledge support of this research by the Department of Energy (DE-FG03-95ER14546) through a grant to J.E.P. Certain commercial equipment, instruments, or materials are identified in this report to specify adequately the experimental procedure. Such identification does not imply recommendation or endorsement by the National Institute of Standards and Technology or the University of Arizona, nor does it imply

(23) Orendorff, C. J.; Ducey, M. W.; Sander, L. C.; Pemberton, J. E. In preparation.

(24) Orendorff, C. J.; Ducey, M. W.; Sander, L. C.; Pemberton, J. E. In preparation.

that the materials or equipment identified are necessarily the best available for the purpose.

#### SUPPORTING INFORMATION AVAILABLE

The Supporting Information contains figures of Raman spectra and plots of the temperature dependence of the  $I[\nu_a(\text{CH}_2)]/I[\nu_s(\text{CH}_2)]$  values and  $\nu_s(\text{CH}_2)$  peak frequencies for those solvents

and stationary phases not shown in the text. This material is available free of charge via the Internet at <http://pubs.acs.org>.

Received for review October 14, 2002. Accepted April 22, 2003.

AC020639G